Renewable Energy 129 (2018) 271–284

Contents lists available at ScienceDirect

Renewable Energy

journal homepage: www.elsevier.com/locate/renene

Laboratory study on the effects of hydro kinetic turbines on hydrodynamics and sediment dynamics

R. Ramírez-Mendoza [a, b, *], L.O. Amoudry [a], P.D. Thorne [a], R.D. Cooke [a], S.J. McLelland [c], L.B. Jordan [c], S.M. Simmons [c], D.R. Parsons [c], L. Murdoch [d]

[a] National Oceanography Centre, 6 Brownlow St., Liverpool L3 5DA, UK
[b] CICESE, Carr. Eda.-Tij. No. 3918, Zona Playitas, Eda., BC 22860, México
[c] University of Hull, Hull HU6 7RX, UK
[d] CFD People LTD, 38 Lyle Road, Airdrie, Glasgow ML6 8NB, UK

ARTICLE INFO

Article history:
Received 22 March 2017
Received in revised form
23 April 2018
Accepted 27 May 2018
Available online 30 May 2018

Keywords:
Energy
Turbines
Tides
Sediment transport

ABSTRACT

The need for hydrokinetic turbine wake characterisation and their environmental impact has led to a number of studies. However, a small number of them have taken into account mobile sediment bed effects. The aim of the present work is to study the impact of the presence of a horizontal-axis three-bladed turbine with the flow and a mobile sediment bed. We use a series of laboratory experiments with a scaled modelled turbine installed in a flume with a mobile sandy bed at the bottom. Acoustic instruments were used to monitor flow, suspended sediment and bed behaviour. Results show a velocity decrease of about 50% throughout the water column and no flow recovery after a distance of 15 rotor diameters. Clearly visible ripples in the absence of the model turbine were replaced by horseshoe-shaped scour pit in the near wake region, and a depositional heap in the far wake. Suspended sediment differences were recorded in the streamwise direction with a possible effect of the wake as far as 15 rotor diameters. These results imply potentially important effects on the efficiency of turbine arrays, if the flow were to be lower than expected, on turbine foundations and modify coastal sediment transport.

1. Introduction

Energy from renewable sources is widely available from water, geothermal heat, sun, wind, biomass and wave-tidal sources. However, their use remains extremely difficult due to conversion processes, limited efficiencies, infrastructure, land availability, systems reliability and environmental impact [1]. In the marine sector, the growing interest in hydro kinetic turbines and tidal stream turbines toward commercial developments requires improved understanding of the implications of array deployments. In particular, the characterisation of the wake of a device is critical for engineering, development and environmental reasons. For hydro kinetic and tidal stream turbines, which aim to extract energy from river and tidal currents, the spacing between turbines in future arrays and thus optimal array design fundamentally depends on the knowledge of the wake recovery length. Environmental effects may include changes to both physical and ecological processes. Examples of such effects are the turbid wakes 30–150 m wide and up to 10 km long which have been observed downstream of offshore wind farm arrays [2,3]. Deployments of tidal stream turbines (TST) could produce similarly large wakes, even though the underpinning mechanisms would be more complicated due, in part, to the combination of a support structure and the moving turbine.

Improved understanding of turbine (hydro kinetic and tidal stream) wakes is fundamentally underpinned by direct measurements both at reduced scales in laboratory flumes and at full scale in the field. These measurements can be, in turn, used to inform and validate the numerical models required to predict the wide-scale implications of turbine deployments (e.g., [4]). Following from their intended purpose, marine tidal stream turbines are expected to be deployed in coastal and shelf seas and in particular in locations with relatively high tidal currents. One implication is that the tidal boundary layer would typically cover the entire water column, another key implication is that wakes generated by TST may then interact with the seabed in these relatively shallow environments.

* Corresponding author. National Oceanography Centre, 6 Brownlow St., Liverpool L3 5DA, UK.
E-mail address: rrmenz@noc.ac.uk (R. Ramírez-Mendoza).

https://doi.org/10.1016/j.renene.2018.05.094

Although laboratory experiments have investigated wakes due to mesh discs [5] and model turbines (e.g. [6,7]), the focus has commonly been on determining the wake recovery length rather than on investigating the impact on environmental physical processes (e.g., [8,9]). Assessing such impacts (on hydrodynamics, waves, turbulence and sediment transport for example) is, however, critical for successful commercial deployments of turbines and has been recognised as a key research gap [10]. Recent experiments have further characterised the wake behaviour in shallow turbulent flow above a fixed bed (e.g. [11]), and investigated near-wall effects and bed shear stress due to scaled turbines above a smooth fixed bed (e.g., [12]). Nevertheless, studies about the complete two-way interactions between the seabed and the presence of the TST remain very scarce.

Deployment of turbines above mobile beds, whether in rivers, estuaries, or the coastal ocean, may lead to a range of issues linked with sediment transport. Generating turbid wakes (e.g. [2,3]), may limit light availability with important ecological consequences. Increased erosion leading to scour can be expected in the near wake of a turbine, although the fate of the eroded sediment is not fully known and the effect on adjacent and nearby turbines is uncertain. Alternatively, other areas may be subjected to net deposition, which may have important ecological and geomorphic implications. The seabed, and changes to it, may also have an important impact on the flow and TST efficiency via the control of bed roughness on the vertical velocity profile. Existing studies that have included artificial roughness (e.g. [5]), have focused on local scour generated by model turbines in laboratory experiments [13], and have measured the interaction between three model turbines and a mobile bed with two-dimensional bedforms [14]. Nevertheless, studies encompassing all elements of the triad of hydrodynamics, sediment bed dynamics and suspended sediment dynamics are still lacking.

This study aims to address this gap and present for the first time an investigation of the interaction between the sediment triad flow, suspended sediment and bed [15], and a modelled turbine using experiments in a flume. We use a set of different acoustic instruments to give a wide covering area of observations for different variables. This will show that the wake due to the scaled turbine has an impact as far as 15 times the diameter of the rotor in the streamwise direction and over the width of the flume. The next Section 2 explains the experimental setup used in this study. Section 3 describes the effects of the modelled turbine on the flow and the sediment bed. The results are discussed in Section 4 in terms of hydrodynamics, wake recovery and the sediment bed. Finally, the main findings are highlighted in the conclusion Section 5.

2. Experimental methods

A series of laboratory scale experiments were carried out in the Total Environment Simulator at the University of Hull, United Kingdom, which was set up as an 11m long and 1.6 m wide flume in order to quantify the potential impact of TST on near-bed hydrodynamics and sediment dynamics (bed and suspended). The effect of a modelled turbine (or rotor) was determined from a comparison between measurements in absence of the rotor and measurements with the rotor installed.

2.1. Scaled laboratory measurements

The interactions between horizontal axis turbines and the triad of hydrodynamics, bed dynamics and suspended sediment dynamics were determined by considering a model three-bladed horizontal axis rotor of diameter $D = 0.2$ m (Fig. 1). The rotor was mounted in a shaft of 8 mm diameter which in turn was attached to a housing of 32 mm diameter with a 25 W DC motor. This allowed

Fig. 1. Tidal stream turbine model used in the experiments with a 0.2 m diameter rotor.

the control of the rotation to a tip speed ratio of 5.5. The housing was fixed to a solid fin of 68 mm × 6mm which was mounted from a gantry above the flume. The experiments were carried out above a mobile bed consisting of a 0.1m thick layer of coarse well-sorted sand (0.41 mm median diameter). The complete particle size distribution is presented in Fig. 2. The flume was filled with freshwater to obtain 0.5 m water column depth. The pumps, which recirculated both sediment and water, were set up to create a steady current approximately 0.5 $m \cdot s^{-1}$. The water and sediment were left to flow in the flume without the rotor until it was considered that the

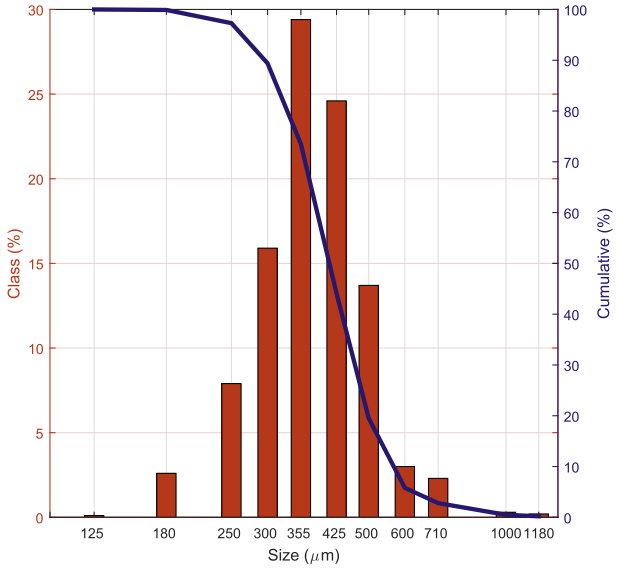

Fig. 2. Particle size distribution and cumulative curve of the sediments used in the experiment.

mobile bed reached equilibrium (i.e. no more evolution of bed form characteristics). This experimental setup resulted in the following non-dimensional summary: the chord-based Reynolds number was approximately 15000, the diameter-based Reynolds number was approximately 10^5, a tip-speed ratio of 5.5 was maintained by a DC motor, a Froude number of 0.22 and a blockage ratio of 0.039. Although two tests were carried out with the rotor centre at 0.15 m and 0.2 m above the no-motion bed location, the rotor centre was placed at the former by default and unless otherwise specified. The no-motion bed location is where the sediment bed was initially in absence of any flow and will be taken as the zero vertical level, i.e. the flume floor was at −0.1 m. Fig. 3 shows a diagram of the flume with the coordinate system used in this investigation. Fig. 4 shows the different horizontal positions of the instruments during the experiments. It is important to note that not all instruments were used simultaneously, because of wakes generated by the instrument housings. Therefore, only one instrument at a time was used at each position. In order to minimize spatial flow inhomogeneity due to flume effects, results are presented as comparison between measurements without the rotor and with the rotor in the flume. In addition, the series of experiments with each instrument without the rotor were taken first and then repeated with the rotor installed in the flume. The results are also compared with previous experiments above a fixed bed made of marine plywood boards.

2.2. Flow measurements

The flow field above the mobile bed was measured using a pulse coherent acoustic Doppler profiler (PC-ADP Nortek Aquadopp HR) mounted in a gantry that allowed changes in the horizontal position of the instrument. The PC-ADP measured vertically downwards from about 0.1 m below the water surface and recorded velocity profiles at 2 Hz sampling rate and in 0.02 m bins of vertical resolution during 10 min at each horizontal location (filled circles in Fig. 4). The flow above the fixed bed was measured using a Nortek ADV with a 25 Hz sampling rate which gave the three velocity components at the same height as the rotor tip (0.2 m above the fixed bed in that case). The ADV was also mounted in a gantry to change the instrument horizontal location (all circles in Fig. 4) and obtained measurements during five minutes at each different location. In this case of the fixed bed experiments Talisman 10 particles were used as velocity seeding material.

Since it is common to obtain spikes in acoustic velocity records due to measurement errors, both data sets above mobile bed and above fixed bed were post processed to remove velocity spikes following the method of Goring and Nikora [16] as modified by Mori et al. [17]. The resulting data sets were then time-averaged to obtain one velocity profile and a single velocity value at each location for the mobile bed and fixed bed, respectively. For the profiler measurements, the space and time varying bed location was estimated from the backscatter intensity and near-bed bins were discarded when not above the bed for all three acoustic beams. Finally, velocity shear was obtained from the vertical profiles as du/dz.

2.3. Sediment bed measurements

The evolution of the sediment bed was measured using a *Marine Electronics* three dimensional acoustic ripple profiler, ARP, [18,19]. The ARP consists of a 1.1 MHz pencil beam transducer mounted on a two axis stepper motor. Looking downward, the system performs vertical profiles describing an arc of about 150° and obtaining a transect of the bed. When the transect was completed, the transducer rotated horizontally 0.9° and collects the next adjacent transect. The sequence was repeated until a complete circular area was scanned. The backscatter profiles were saved and a bed

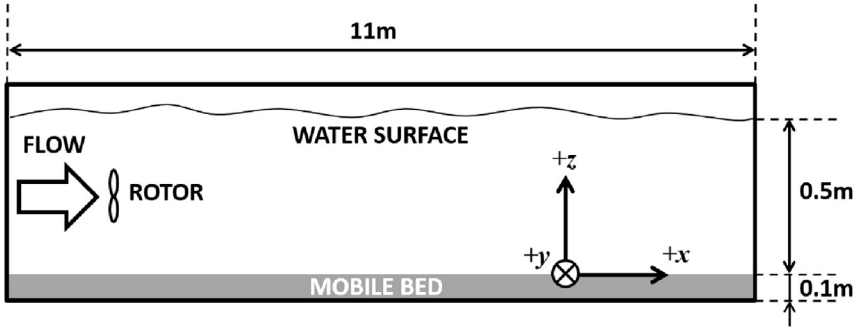

Fig. 3. Side view scheme of the flume with the model turbine and coordinates used in this study. Rotor height over the sediment bed is 0.15 m unless otherwise is specified for a particular case. Drawings not to scale.

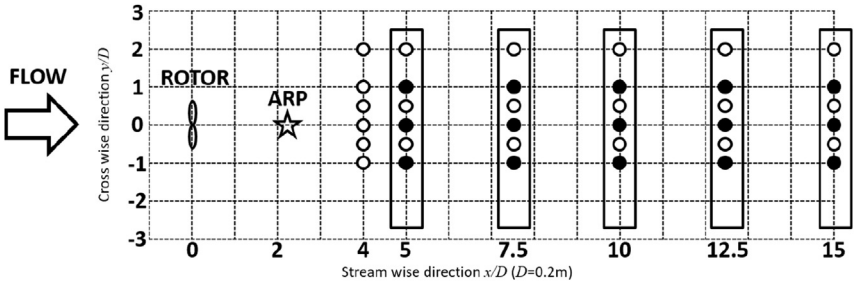

Fig. 4. Measurement locations (rotor diameter $D = 0.2$ m). i) Filled circles indicate locations of velocity profiles above the mobile bed, ii) all circles indicate locations of velocities above the fixed bed used for comparison, iii) star symbol indicates the acoustic ripple profiler ARP, location and iv) continuous lines indicate suspended sediment concentration measurement locations. Rotor position is at 0,0 location.

recognition algorithm was used to locate the position of the bed relative to the transducer which was then converted to surface bed heights relative to the flume floor.

For the experiments in this study, the ARP was mounted at a fixed position in the horizontal plane at 0.43 m downstream from the turbine and completed the circular area in about 12 min. This circular area was larger than the flume width and therefore a square central section of 1.4 m^2 was extracted for the analysis. This area was 0.2 m smaller than the flume width to avoid the effects of the walls on the echo signal. An ARP measurement was taken with the flume filled with water but without flow to record acoustic background levels which were subtracted from experiment measurements. Time series of bed evolution were collected with the rotor at two heights from the bed, 0.15 m and 0.2 m, in order to study the short-term (hours) effect of TST deployment height on the sediment bed. A last ARP measurement was taken at the end of all the experiments to obtain the final bed morphology.

2.4. Suspended sediment measurements

Suspended sediment concentrations were obtained using a BASSI Instrument [19], which is a version of an acoustic backscatter system (ABS). The BASSI (Bedform and Suspended Sediment Imager) consists of three transducer line arrays aligned to give a plane view of the backscattering in the flow. For the present study, two arrays were used with 15 transducers each with five groupings of three adjacent transducers operating at frequencies of 0.75, 1.25 and 2.5 MHz. Backscattering vertical profiles were recorded at about 5 Hz sample rate during at least 10 min on five streamwise locations (Fig. 4). The profiles were then time-averaged to obtain a single vertical profile for each transducer. Based on the scattering properties of sand sediments and the three different frequencies used, the mass concentration of suspended sediments were calculated following Thorne and Meral [20] and Moate et al. [19]. Suspended sediment concentrations (SSC) of each three transducers (three frequencies) were then averaged to give a single vertical profile representative of each three transducers locations.

3. Results

3.1. Mobile bed effect on the flow

Vertical velocity profiles of the along-flume component, U, when the bed consisted of a sand layer are shown in Fig. 5. The profiles with and without the rotor in the flume are shown as open red and blue circles respectively. All the profiles with and without rotor showed similar structure consistent with boundary layer velocity profiles (discussed later). However, with the only exception of the $x/D = 5$, y/D $= -1$ location, all profiles showed important velocity decrease with variable magnitudes. At $x/D = 12.5$, $y/D = -1$ the velocity decrease was about 0.1 $m \cdot s^{-1}$ while at $x/D = 10$, $y/D = 1$ of 0.3 $m \cdot s^{-1}$. Overall, the profiles at $y/D = -1$ location were the least affected by the presence of the rotor and the most affected were the profiles in the far wake from $x/D = 10$ streamwise and both $y/D = 0$ and $y/D = 1$ crosswise locations. It is important to note that zero level in Fig. 5 corresponds to the no-motion bed location and all the profiles shown stop slightly higher because the ripples affect the acoustic signal and the first bins close to the surface sediment bed had to be discarded. It is also clear that the presence of the rotor increases even more the bed effect and more bins near the bed were discarded, implying changes to the mobile sediment bed.

The shear velocity profile structure is similar with and without the rotor in most of the water column (Fig. 6). Shear values remained low (<1 s^{-1}) near the surface and increased towards the bottom to around 2 s^{-1}. The variability along the profiles remained high without clear differences between both cases with and without rotor.

3.2. Fixed bed flow characterisation

Results from the ADV point measurements (rotor and ADV at 0.2 m above the bed) are presented in Fig. 7 for the mean velocity in the streamwise (U) direction, displaying the ratio of the mean velocity measured with the scaled turbine (U_{fix}) normalised by the mean velocity measured at $x/D = 0$, $y/D = 0$ location in absence of scaled turbine (U_{ofix}). A value of one indicates no change due to the presence of the turbine, while values above/below one indicate increased/decreased velocities due to the rotor. It can be seen that the greater effects were found in the near wake region with velocity reductions of about 20% and 25% at five and four diameters from the rotor, respectively. However, these effects were limited to the area directly behind the rotor, i. e. $y/D = 0$ and $y/D = -1$ in the cross wise direction. In contrast, velocity reductions in the range of 5%–10% were obtained in far wake regions in both cross wise and streamwise directions. A slight velocity increase in the positive side of the channel was recorded at all locations. The spatial resolution is low for these experiments as their only purpose was to compare the general features with the mobile bed experiment results.

3.3. Bed evolution

The long-term changes in the sediment bed at the beginning and end of the experiments are shown in Fig. 8. The initial state showed ripples in the sediment bed of about 0.3 m long and evenly distributed over the measurement area (Fig. 8a). A slight bed height difference between the negative and positive sides (crosswise direction) of the flow was present with the latter higher than the former. The difference between mean heights at both sides was less than 0.03 m and is due to small variations in the initial sediment bed. After the experiments with the rotor at 0.15 m above the no-motion bed were carried out the ripples were replaced by scour in the near wake and increased deposition in the middle (Fig. 8b). A small area to the positive side of the flow, $+ y/D$, still presented flow orientated ripples while the negative side showed ripples that may be a result of the rotor wake. There is an overall shift towards higher elevations after the experiments (lighter colour in Fig. 8b), which implies sediment deposition was the dominant factor in the measured area. The sediment bed mass change was estimated from the change in bed position (elevation) from the pre-experiment bed (Fig. 8a) to the post-experiment bed (Fig. 8b). Each interpolated area by the ripple profiler corresponds to approximately 2.3×10^{-5} m^2 and the sand density is assumed to be 2650 $kg \cdot m^3$. This mass change is then split in deposition and erosion: 68.5 kg were deposited and 7.7 kg eroded, leading to a net gain/deposition of 60.8 kg. Since all the experiments were carried out during working hours each day, the effective time that the flow was running in the flume was about 48 h which gave a rough estimate of the deposition rate of 1.2 $kg \cdot hr^{-1}$.

Fig. 9 shows the changes of the sediment bed at the streamwise flume centre line throughout the experiment using the acoustic ripple profiler with the rotor centre at two different positions: 0.2 and 0.15 m above no-motion bed (mab). Two ripples of about 0.05 m crest height are clearly visible in the initial profile at 10:55. The crest of the first ripple is located before the rotor and remained almost unchanged during the experiment until 12:57. The crest of the second ripple was behind the rotor at about $x/D = 2.8$ although was not clearly visible at 11:19 because of the important sediment transport around this location and $x/D = 5$. The crest was followed

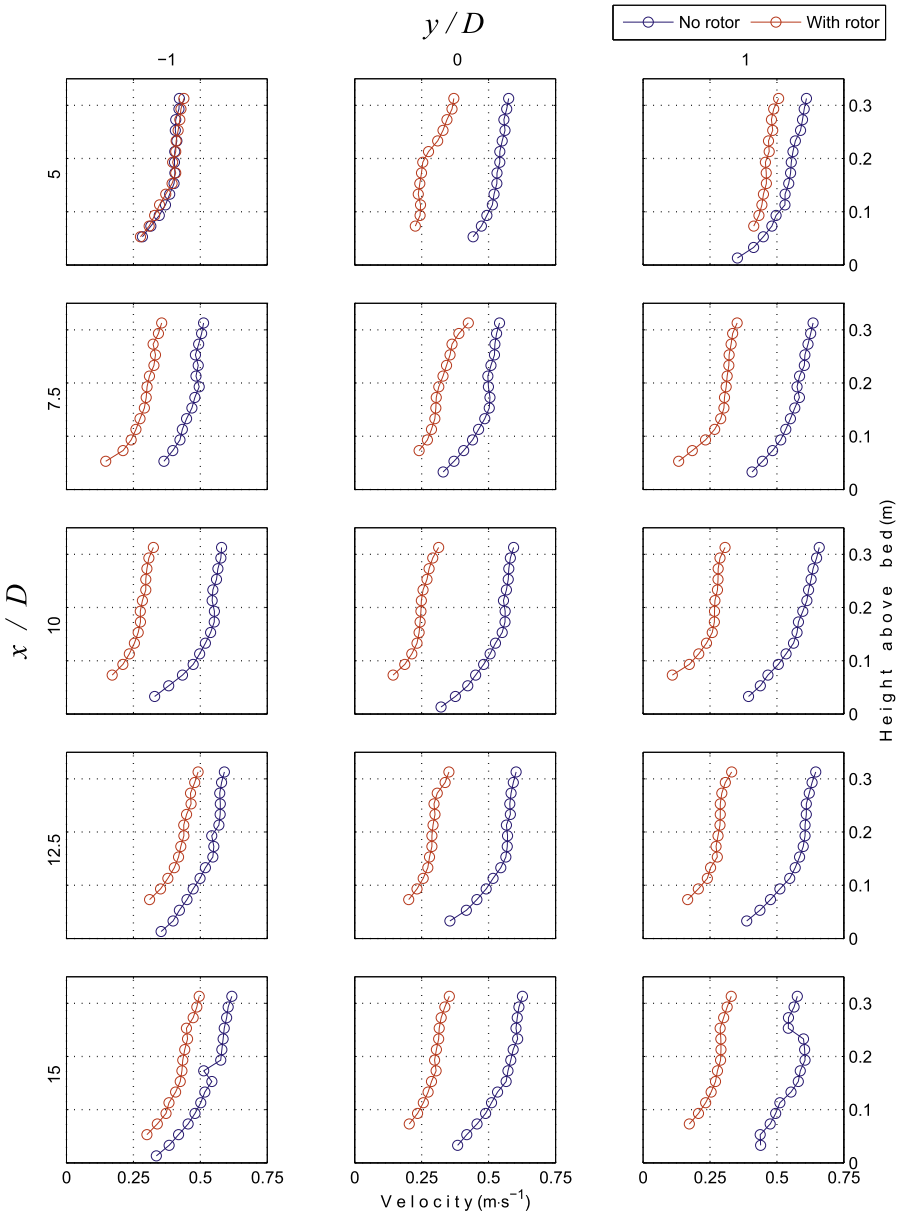

Fig. 5. Profiles of streamwise velocity component (U). Upper and left numbers indicate the horizontal position of each profile relative to rotor diameters D. Red and blue open circles are profiles with and without the rotor in the flume, respectively. The rotor was installed horizontally at $x/D = 0$,$y/D = 0$ stream and cross wise directions, respectively. The zero level on the vertical right axis is the no-motion sediment bed location (initial condition). (For interpretation of the references to colour in this figure legend, the reader is referred to the Web version of this article.)

by an increase in bed height at $x/D = 5$, which also showed significant changes during the experiment. This crest was not visible at 12:57 due to sediment deposition from $x/D = 3$ to 5 locations. The strongest effect of the rotor during the experiment at 0.2 mab was on the near wake region between $x/D = 0$ and 2 which presented significant erosion and even forming a plane section at 11:44. At the end of this experiment (12:57) a new crest appeared at $x/D = 4.8$ and reached almost 0.1 m in height. A different behaviour was found when the rotor was lowered to 0.15 mab. As expected the erosion was increased and a depression developed in the near wake region that was deeper but shorter than in the 0.2 m case. Unlike the 0.2 m case there were small ripples formed in the far wake region and the overall morphology changed more than for the case with rotor at 0.2 mab. The first three profiles (13:28–13:53) showed small ripples behind the scour to $x/D = 5$ location. A clear crest formed in the next three profiles (14:06–14:35) around the $x/D = 2$ location and also ripples in the far wake area in profiles 14:19 and 14:35. These were replaced by small ripples at 15:05 and a crest seemed to form again in the next profile after the $x/D = 2$ location. However, the small ripples behind the scour were the characteristic bed form in the last two profiles.

3.4. Suspended sediments

The logarithm of the SSC obtained in $kg \cdot m^{-3}$ is shown in Figs. 10 and 11 for the conditions without the rotor and with the rotor in the flume, respectively. There is a resuspension of sediments without the rotor which is the normal response in the flume. Without the rotor, more sediments are in suspension at 5D than at 15D along the channel locations and also there is a slight cross channel difference

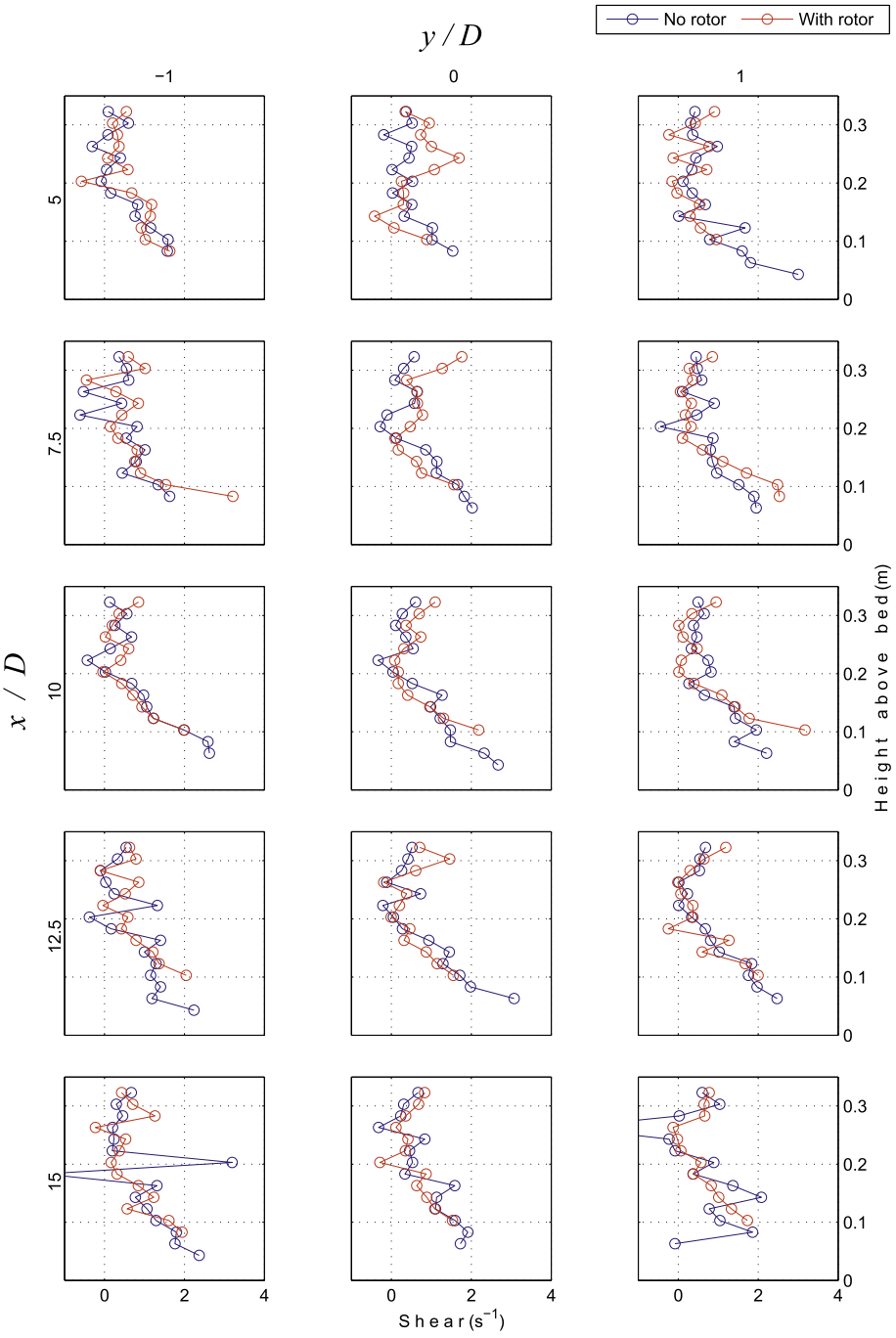

Fig. 6. Shear velocity profiles of the streamwise flow component. Upper and left numbers indicate the horizontal position of each profile relative to turbine diameters *D*. Blue lines show shear velocity without rotor and red lines with the rotor in the flume. The model turbine was installed horizontally at $x/D = 0$, $y/D = 0$ stream and cross wise directions respectively. The zero level on the vertical right axis is the no-motion sediment bed location (initial condition). (For interpretation of the references to colour in this figure legend, the reader is referred to the Web version of this article.)

with more sediment resuspended at the negative side of the flume ($-y/D$). This may be due to the bedforms affecting sediment resuspension in both the streamwise and the cross stream directions. When the rotor is in the flume (Fig. 11) more sediments are resuspended near the bed with the highest concentrations at 5*D* cross channel location. Concentration diminished near the bed at 7.5*D* but suspended sediments were transported higher into the water column. At the 10*D* location suspended sediment concentration diminished but was still higher than the no rotor experiments case at the same location. Suspended concentration remained almost the same at 12.5*D* but increased again in the far wake region at 15*D*.

4. Discussion

4.1. Hydrodynamics

The presence of the model turbine in the flume affected the flow above the fixed bed mostly following expectations (see Fig. 7). A wake was generated and the results are qualitatively consistent

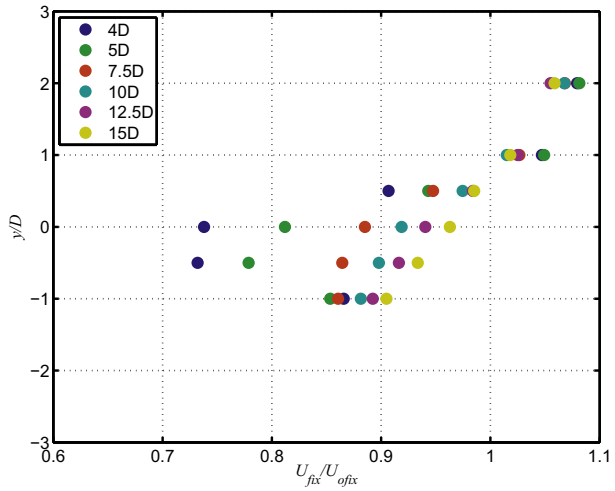

Fig. 7. Fixed bed rotor wake for mean streamwise velocity; U_{fix} is the mean velocity with the scaled turbine installed at 0.2 m above bed, U_{ofix} is the mean velocity at $x/D = 0$, $y/D = 0$ in absence of the rotor. Different colours correspond to different distances downstream of the model turbine relative to rotor diameters as shown in the legend. (For interpretation of the references to colour in this figure legend, the reader is referred to the Web version of this article.)

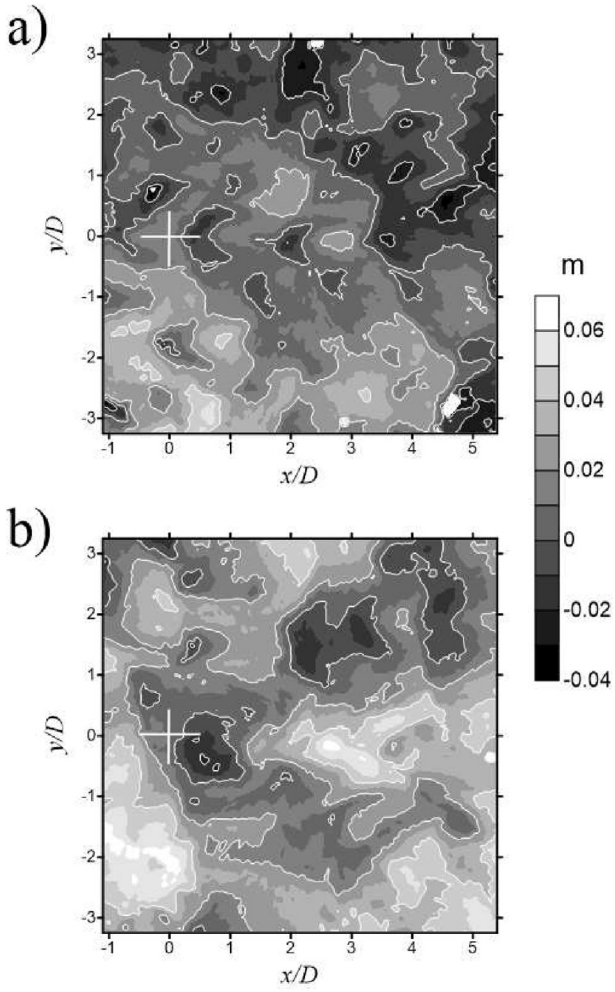

Fig. 8. Sediment bed comparison. a) Before the experiments and b) after the experiments with the rotor centre at 0.15 m above sediment bed. Rotor position is indicated by the white plus sign.

with previous flume studies: some level of asymmetry and the wake recovery are similar to the results of Tedds et al. [21]. We can also see some widening of the wake going downstream of the model turbine, as would be expected for a self-similar wake, and as observed by Stallard et al. [11]. The wake recovery is tested against the behaviour of self-similar axisymmetric and plane wakes in the next section.

The effect of the mobile bed only on the flow is the presence of an important shear which covers almost the entire measured water column. When the rotor was also in the flume, velocity magnitudes decreased about 50%. A similar boundary layer developed in both cases with and without the rotor in the flume describing a rough wall log-law. Friction velocity (U_f) and bed roughness (z_0) were calculated from the linear fit of the wall log-law:

$$U = \frac{U_f}{\kappa} ln \frac{z}{z_0} \tag{1}$$

where U is the flow velocity in the flume, κ is the von Karman constant (0.41) and z is height above bottom. Fig. 12 shows the measured velocity profiles (open circles) and calculated profiles from the law of the wall (solid lines) for both with and without the rotor in the flume. Table 1 shows the corresponding values for U_f and z_o from the linear fit.

Also included in Fig. 12 are the calculated velocity profiles corresponding to a (1/7)th power law (dashed lines):

$$U = U_r \left(\frac{z}{z_r}\right)^{1/7} \tag{2}$$

where U is the calculated velocity at the height z based on the velocity reference U_r at a reference height z_r which for this case is the rotor height. Most of the calculated velocity profiles adjust well to a log law for both with and without the rotor. In contrast the (1/7)th power law slightly overestimates the velocity near the bottom when the rotor was not in the flume while the overestimation increases when the rotor is present. The bed roughness z_0 and friction velocity U_f presented spatial differences. The side corresponding to the $y/D = 1$ location showed higher friction velocities with the rotor in the flume while there was no specific pattern for the central part and $y/D = -1$ locations. For the bed roughness, the values at the $x/D = 5$ location were similar for both with and without the rotor while higher bed roughness were calculated for streamwise from $x/D = 7.5$ to 15 and all crosswise locations when the rotor was installed in the flume. This means that a more dynamic bed resulted from the installation of the rotor. Unlike the results by Myers and Bahaj [5]; which showed only slight differences in vertical profiles of streamwise velocity for smooth and rough beds, this study shows important differences when a mobile bed is present. Another important fact is that no flow recovery is reached after 15 diameters from the rotor location. This represents a significant difference in comparison with experiments over fixed beds and could have important implications for the design and installation of marine turbines. It is noteworthy that the velocity reduction due to the wake seems to be more important above the mobile bed. This means experiments using fixed beds probably underestimate the flow deficit. In addition, the lack of recovery should be accounted for in the design of rotor arrays.

The similar structure in the shear profiles shown in Fig. 6 is an unexpected result. According to these profiles the sediment is taken into suspension equally with and without rotor in the flume. Therefore, horizontal advection is the most important process for sediment transport and the changes to the streamwise velocity because of the rotor were the most significant in these

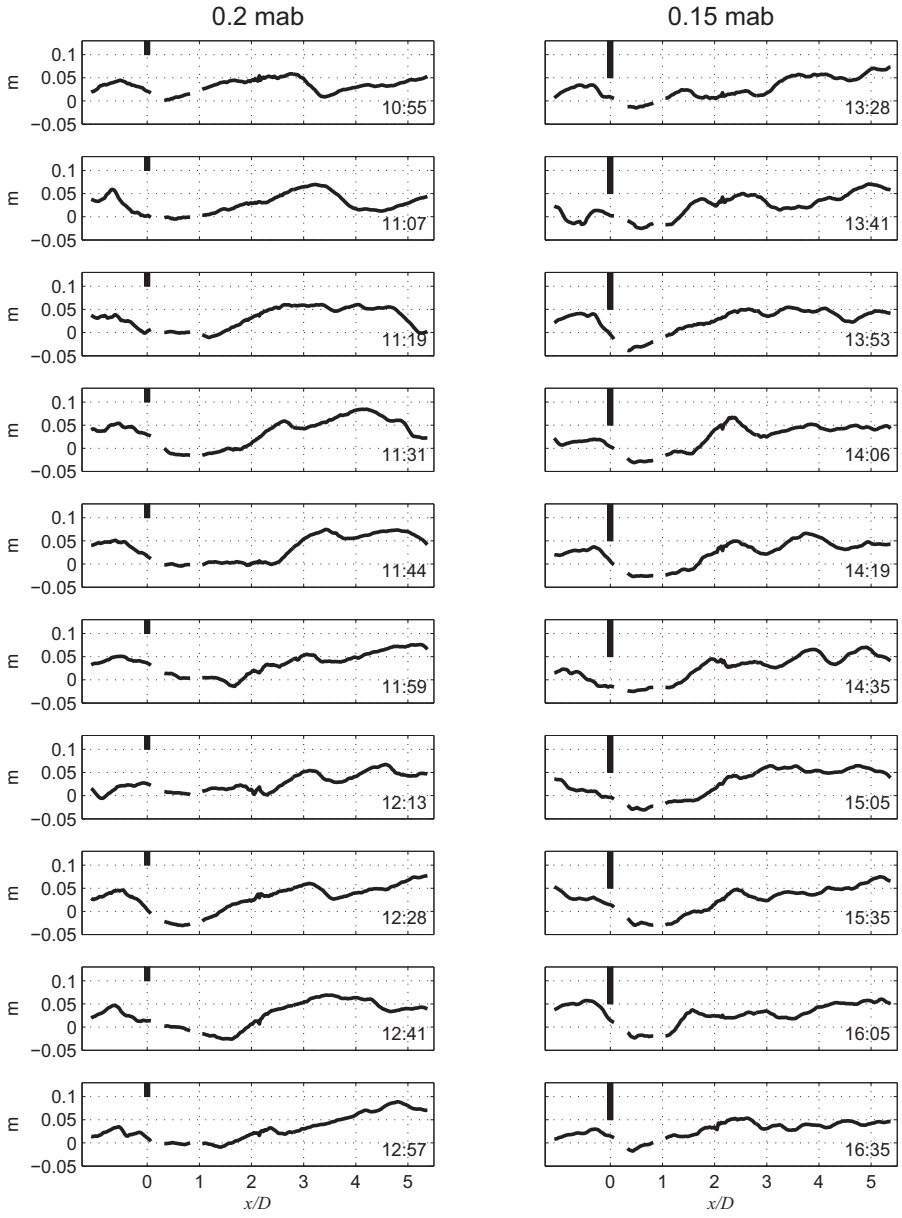

Fig. 9. Streamwise horizontal profiles of the sediment bed along the central part of the measured area. Left panels show bed evolution with rotor centre at 0.2 mab (metres above bed) while right panels show bed evolution with rotor centre at 0.15 mab. Flow from left to right and rotor is at $x/D = 0$ location with the rotor tip showed by vertical black lines at 0.1 and 0.05 mab. Time in hours and minutes (hh:mm) is indicated by the lower right numbers on each panel. Line discontinuities are locations of acoustic signal reflections which have been removed.

experiments. These results were obtained in the far wake area, from the $x/D = 5$ location, and could be different in the near wake area shown in Fig. 8. It should be noted that the profiles with the rotor present in the flume are shorter than the profiles without rotor. It is possible that increased turbulence affected the acoustic signal of the aquadopp bins near the bed and were discarded during profile processing. These near bed bins could have higher shear and maybe evidence of bed load sediment transport. This remarks on the difficulty of measuring very close to the bottom in a mobile bed and the need for accurate measurements to quantify the interactions of the bedforms and turbulence [22] accounting for the presence of a tidal turbine.

A relevant result is the velocity difference along the crosswise direction of the wake due to the rotor despite the controlled conditions in the flume. For example, as shown in Fig. 5, the most important velocity decrease was found at $x/D = 5$, $y/D = 0$ location, while the $x/D = 5$, $y/D = 1$ presented a slight velocity decrease and the velocity at $x/D = 5$, $y/D = -1$ remained at the value of the no-rotor condition, i.e. no effect of the rotor. The differences may be the effect of the wake developing in a spiral form along the flume and therefore giving different velocity magnitudes in both along and cross channel directions. This would have obvious implications in sediment transport as can be seen in Fig. 8b. Under normal conditions ripples are present in the entire measured area. The pattern changes with the rotor causing erosion from the near wake centre line region and spreading to the far wake area in a horse shoe shape while deposition is present from about $x/D = 2$ to the far wake area. Nevertheless, the magnitude of erosion/deposition is

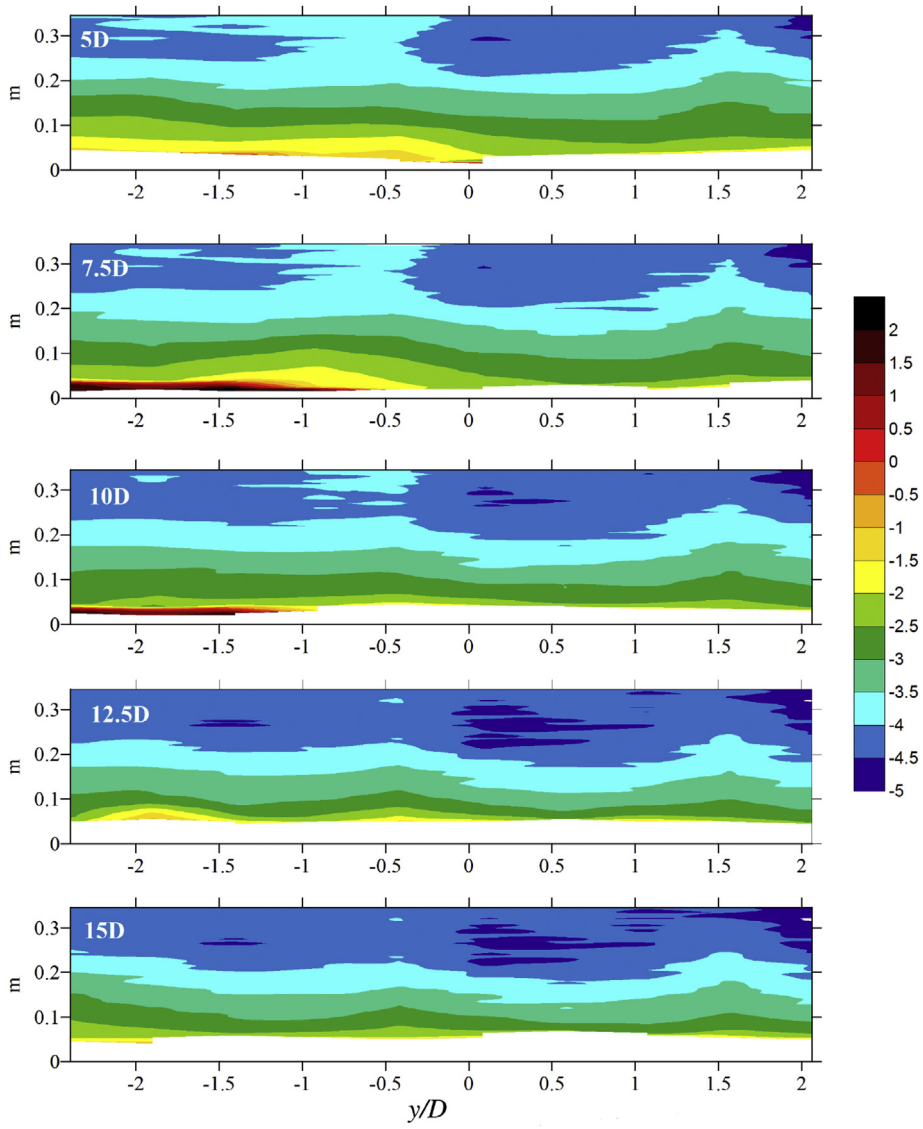

Fig. 10. Cross channel panels of logarithm of the suspended sediment concentration (SSC in kg·m^{-3}) without the rotor. Distance from the rotor is indicated in the upper left corner on each panel relative to rotor diameters.

not the same at both sides of the centre line with more sediments to the negative side of the flow.

To the authors knowledge, with the exception of the work of Hill et al. [14]; the interaction between the flow and a turbine in the presence of a mobile bed has not been investigated experimentally before. Although there are a number of studies about bed morphology and flow (e.g. Refs. [22–24]), they are focused on the effect of the flow over bedforms. Hill et al. [13] studied the scour caused by a model turbine but the changes in the flow were not measured. The study of Hill et al. [14] took into account the changes in turbine efficiency due to bedforms caused by sediment transport. The turbine efficiency diminished because of the bed morphology effects on the flow which is in agreement with the findings in this investigation. Even though the experiments by Myers and Bahaj [5] are different to the experiments in this study, the authors also found an effect of the bed on the flow. Their study shows an increased velocity deficit due to the rotor turbulent wake merging with the turbulent bed boundary layer. This highlights the need for more experiments to assess the interactions between the seabed, the flow and the turbine/rotor.

4.2. Wake recovery

The effects of both rotor and mobile bed can be identified more clearly by comparing the flow before and after their placement in the flume. Fig. 13 shows the centreline streamwise mean velocity ($y/D = 0$) at far wake locations from experiments with fixed bed to mobile bed with the TST model in the flume (middle panel). The flow velocity with fixed bed only (red circles) remained almost constant with a decrease of about 0.025 m·s^{-1}. The presence of the rotor resulted in a flow decrease similar to a number of previous studies (e.g. Refs. [6,7,9], and almost complete recovery at $x/D = 15$ location. This will be discussed in more detail below. The effect of the sediment bed can be clearly seen slightly increasing the flow velocity (blue circles). However, an important decrease resulted from the deployment of the rotor and without clear recovery (green circles). In the experiment with only the sediment bed in the flume, the flow showed recovery at both measured sides from the centreline, first and third panels in Fig. 13. Nevertheless, the flow velocity decreased in a significant way with the addition of the rotor in the flume. There seems to be a recovery at $y/D = -1$ but may be

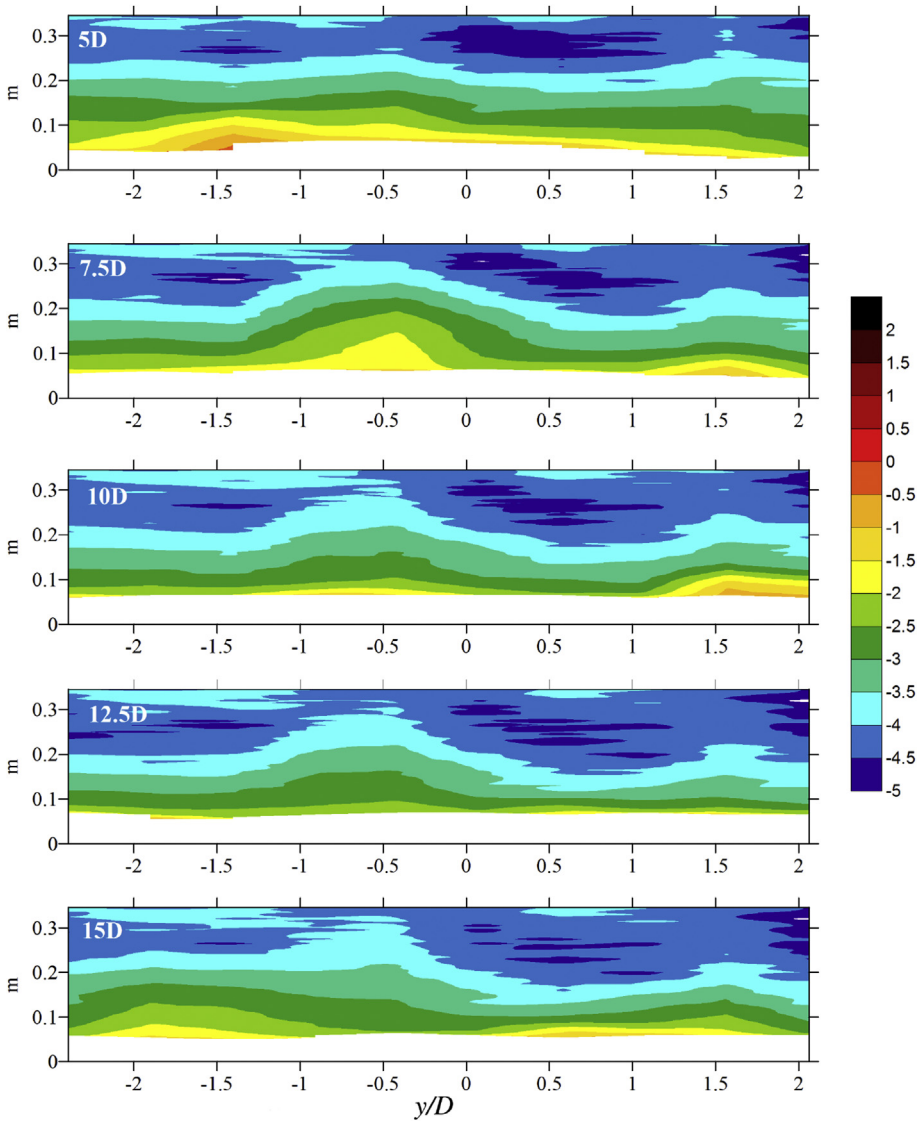

Fig. 11. Cross channel panels of logarithm of the suspended sediment concentration (SSC in kg·m^{-3}) with the rotor installed in the flume. Distance from the rotor is indicated in the upper left corner on each panel relative to rotor diameters.

the result of the high flow variability on this particular side of the flume. Unfortunately, no measurements were obtained at the sides of the flume for the case of the fixed bed due to instrument malfunction.

In order to compare the wake recovery above the fixed bed with that above the mobile bed, we calculate and present the velocity deficit along the centreline of the rotor from the ADV mean velocities. We define the velocity deficit as:

$$\Delta U_{cfix} = \left| U_{fix} - U_{ofix} \right| \tag{3}$$

$$\Delta U_{cmob} = |U_{mob} - U_{omob}| \tag{4}$$

where the subscripts *fix* and *mob* are for the fixed and mobile bed experiments, respectively. Mean velocities with the rotor at the centre line are U_{fix} and U_{mob} while mean velocities without the scaled turbine in the flume are U_{ofix} and U_{omob}. Fig. 14 shows the velocity deficit for both mobile bed and fixed bed experiments, the latter case is also compared to the theoretical behaviour for plane wakes and axisymmetric wakes. For plane wakes the maximum/centreline deficit diminishes with distance downstream as $x^{-1/2}$ in the far wake when the flow becomes self-similar. For axisymmetric wakes, the velocity deficit varies as $x^{-2/3}$ in the self-similar region. Both theoretical behaviours shown in the figure are a best fit to the experimental data, which resulted in the following relationships:

$$\frac{\Delta U_{cfix}}{U_{ofix}} = 0.90\left(\frac{x}{D}\right)^{-1/2} - 0.21 \tag{5}$$

and

$$\frac{\Delta U_{cfix}}{U_{ofix}} = 0.95\left(\frac{x}{D}\right)^{-2/3} - 0.13 \tag{6}$$

in which the results at $x/D = 4$ downstream locations are discarded because they are probably not located in the self-similar region. The fit to an axisymmetric wake results in smaller errors (RMSE value of 0.048 versus 0.067 for the plane wake). These results are consistent with previous studies with respect to plane wake behaviour (e.g.

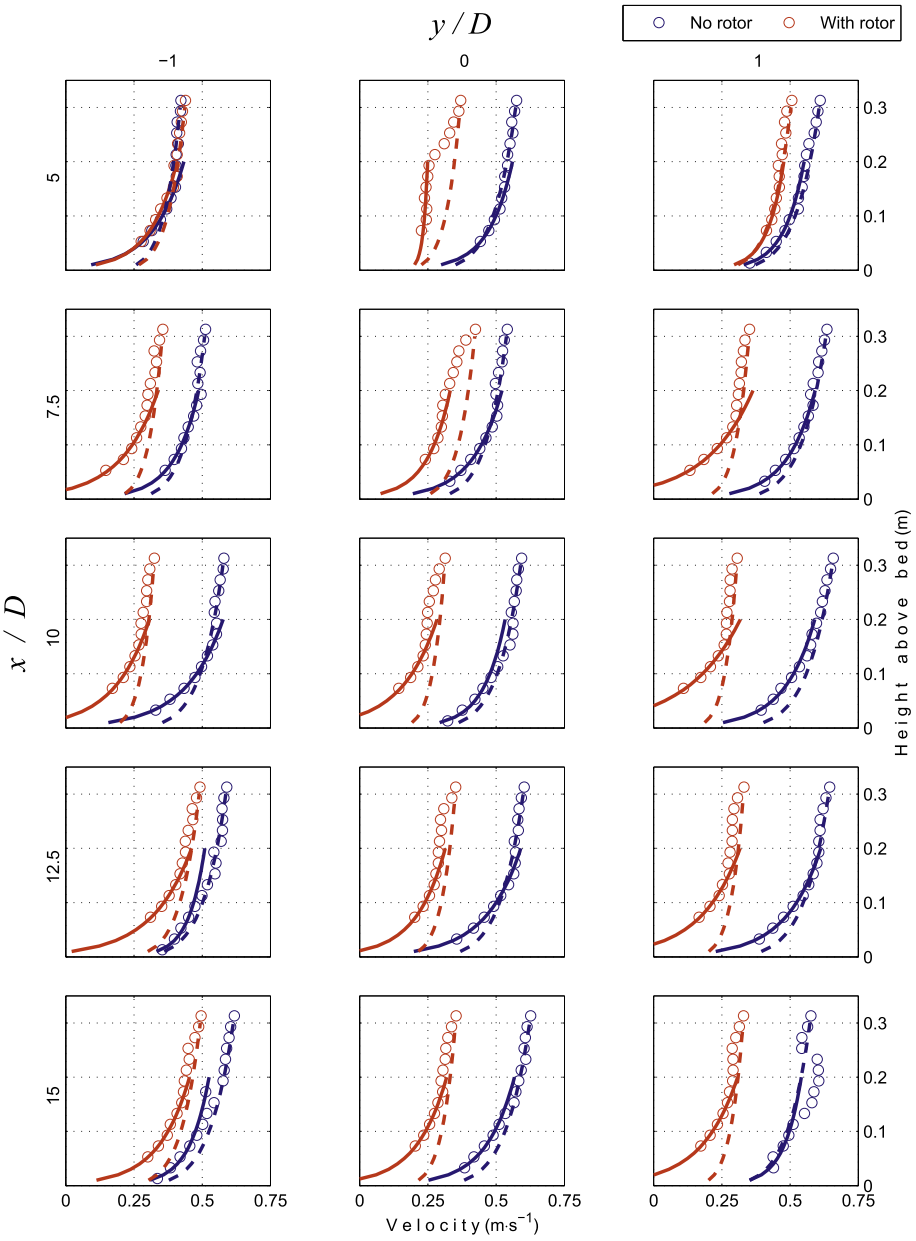

Fig. 12. Measured velocity profiles (circles), calculated profiles based on a log law approximation (solid lines), Eq. (1), and calculated profiles based on a 1/7th power law approximation (dashed lines), Eq. (2). Blue and red colours correspond to without the rotor and with the rotor in the flume, respectively. (For interpretation of the references to colour in this figure legend, the reader is referred to the Web version of this article.)

Table 1
Friction velocity U_f ($cm \cdot s^{-1}$) and bed roughness z_o (mm) obtained from the linear fit to the log law for the measurements of both experiments with and without the rotor installed in the flume.

		$y/D=-1$		$y/D=0$		$y/D=1$	
		No rotor	Rotor	No rotor	Rotor	No rotor	Rotor
$x/D=5$	U_f	4.6	4.0	3.5	0.6	3.0	2.4
	z_o	4.3	0.3	0.3	0.0	0.1	0.0
$x/D=7.5$	U_f	3.7	5.6	4.4	3.4	4.3	7.1
	z_o	0.9	1.6	1.6	0.4	0.7	2.4
$x/D=10$	U_f	5.7	5.3	3.2	5.4	4.5	8.1
	z_o	3.2	1.9	0.2	2.3	1.0	4.0
$x/D=12.5$	U_f	2.4	6.0	5.3	4.4	5.2	5.9
	z_o	0.0	0.8	2.1	1.0	1.6	2.2
$x/D=15$	U_f	2.9	4.6	4.0	4.5	2.5	5.4
	z_o	0.1	0.3	0.9	1.1	0.0	1.9

[11]), but also indicate that an axisymmetric wake behaviour is a better representation of the turbine wake.

The wake recovery is drastically different above the mobile bed compared with the fixed bed. The combination of mobile bed and the rotor presence significantly modified the flow, which implies that the presence of the rotor had a more significant effect above the mobile bed. Velocity deficit remained high along the entire measured transect (from 4 to 15 diameters downstream) and there was little wake recovery observed above the mobile bed even after 15 diameters.

4.3. Bed morphology

Several changes in bed morphology have been found in the present investigation. The clearest feature is the scour in the near

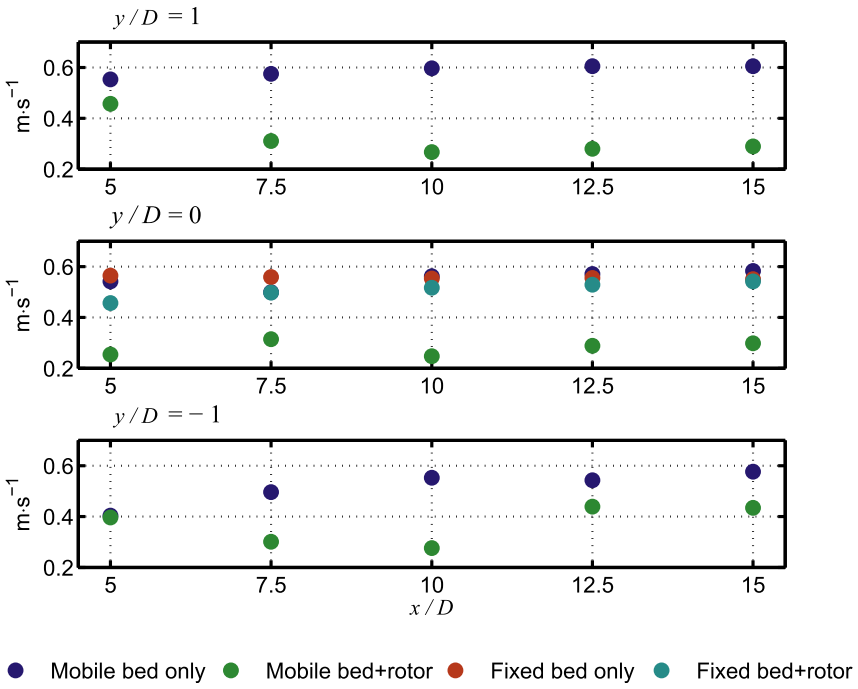

Fig. 13. Streamwise velocity comparison with only the mobile bed and with the rotor in the flume at three y/D locations. At the centre line, middle panel, also the fixed bed results are included.

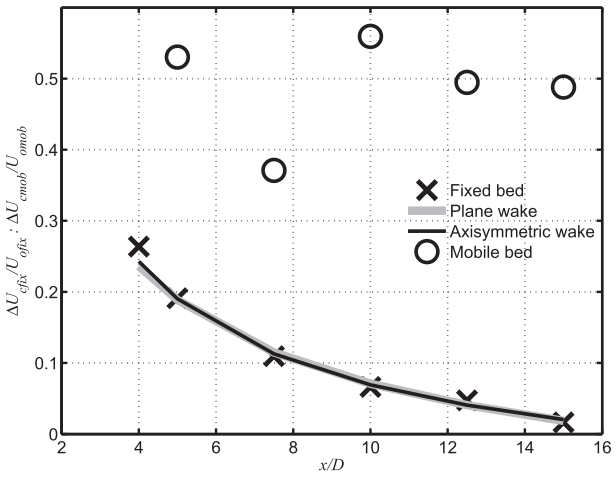

Fig. 14. Streamwise velocity deficit at the centreline of the flume. Symbols denote measurements while solid gray and black lines are the best fit to Eqs. (5) and (6).

wake area. Scouring occurs immediately after the rotor and seems to remain during the entire experiment. This scour pit deepens and shortens when the rotor is closer to the bed. An increase in bed shear stress just below the turbine, as found by Möller et al. [12] is the most likely cause. The experiments of Hill et al. [14] also showed similar scour but it may have been produced by a support structure in that case. Indeed in an earlier study by Hill et al. [13]; the foundation of the rotor seemed to play an important role in the bed scour.

The presence of ripples is a common morphological feature in our experiments. In contrast to scour, which seems to reach a rapid equilibrium, bed morphology remains in constant change as ripples migrate and sediment is transported along the flume. When the rotor is closer to the bed, the scour effect is more localised and this appears to allow the formation of ripples in the downstream wake area after a distance of two rotor diameters. These morphology features were seen by Hill et al. [14] using higher velocity and large sediment size which indicates this can be a common result to take into account in tidal turbine deployments. In particular, sediment deposition in the far wake area shown by this study and also found by Hill et al. [13] would be an important factor for the installation of downstream aligned turbine arrays.

4.4. Suspended sediments

Sediment resuspension showed an unexpected behaviour in the far wake region. The highest concentration was found to the negative side of the flume at 5D (Fig. 11, first panel). The wake seems to have more influence afterwards increasing the sediment in some areas but decreasing in others (7.5D). Further away, the magnitude decreases but the difference between both sides is still clear which implies crosswise asymmetry of the mobile bed due to the rotor. Even though there are differences in resuspension patterns without the rotor shown in Fig. 10, the resulting flow due to the rotor changes the conditions of erosion and deposition in the flume. This is clearer in Fig. 15, where the effect of the presence of the rotor on the suspended sediment is isolated by plotting the ratio C/C_o, where C is SSC with the rotor present while C_o is SSC without rotor. Overall, more sediment was resuspended with the rotor in the flume. High concentrations were found near the bottom at 5D while similar high concentrations were found in upper levels of the water column at 7.5D (second panel) and $y/D = -0.5$. Such mid-water column peaks in SSC have also been observed in the field in the wakes of offshore wind farms [2]. At 10D (third panel) the highest concentrations were present at $y/D = 1.5$ and 2 in the crosswise direction. At 12.5D and 15D the increase in sediment resuspension is still visible. The characteristic feature of the suspended sediment is the non-homogeneous change in both directions in the flume.

An interesting result of the present study is the increase in SSC even though flow velocity decreased about 50% with the rotor

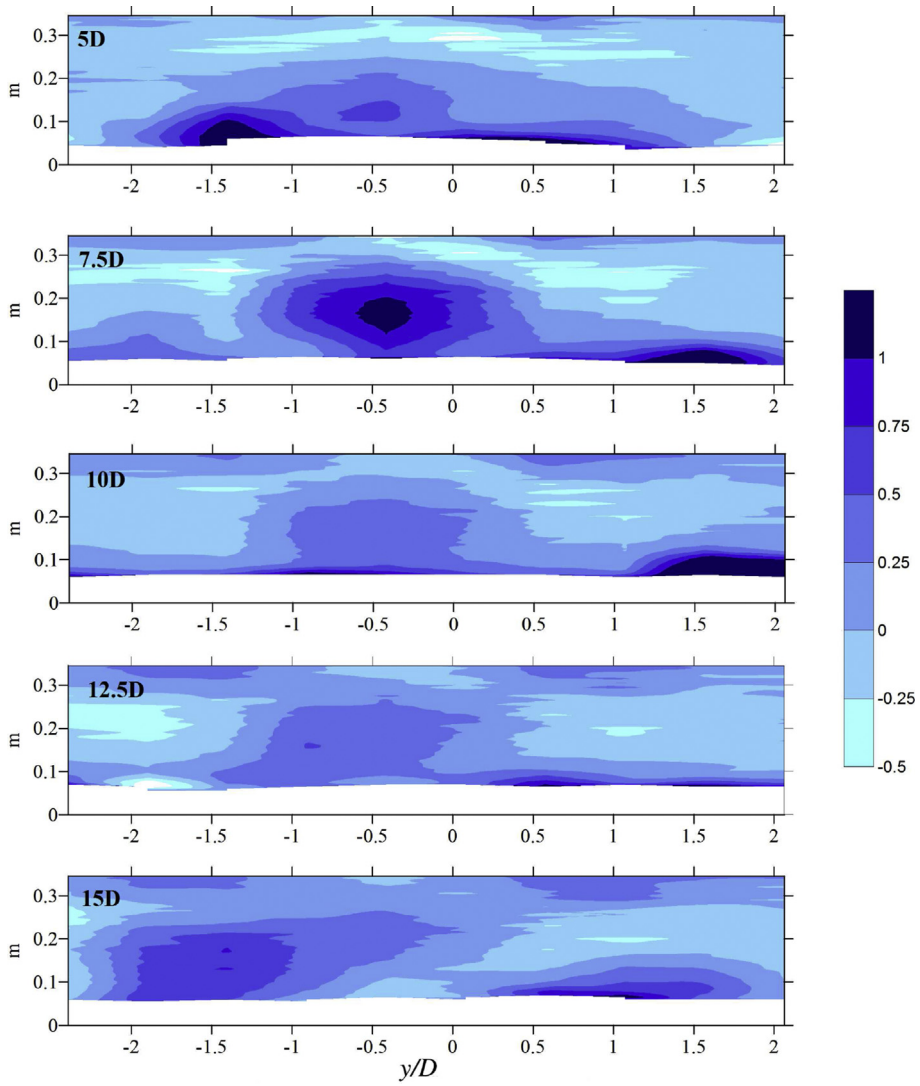

Fig. 15. Cross channel panels of the logarithm of the ratio C/C_o, where C and C_o are SSC with and without the rotor in the flume, respectively. Distance from the rotor is indicated in the upper left corner on each panel relative to rotor diameters.

installed in the flume. The localised sites of high SSC shown in Fig. 15 are evidence of increased bed shear stress. However, our measurements could not resolve shear stresses closer to the bed than those shown in Fig. 6. The effect of the ripples reflecting the acoustic signal is likely the cause of contamination and loss of the velocity bins in close proximity to the bed. This highlights again the importance of more investigations using instruments or techniques capable to take measurements close to the bed.

It is possible that the asymmetry effects previously reported were enhanced in our experiments leading to clear differences in deposition-erosion rates in the measured area. Unfortunately, to the authors knowledge, there is no other study attempting to include together three-dimensional changes of the three key factors: flow, sediment bed and suspended sediments due to the presence of a tidal stream turbine. This means the interaction between the sediment bed and hydrodynamic properties needs further investigation to be properly implemented in coastal numerical models under real conditions.

5. Conclusion

A series of experiments were carried out in the Total Environment Simulator flume at the University of Hull, UK. The use of acoustic instruments allowed characterisation of the three-dimensional interaction between the wake of a scaled turbine, flow, and a mobile sediment bed. Characterisation of the flow over a fixed bed was also carried out and reproduced the typical velocity decrease in the near wake area with recovery in the far wake area. However, recovery varied in the cross wise direction, even displaying velocity increase at some far side locations. This lateral variability may be due to different spatial effects of the wake related to the gyre rotation of the turbine. Above a mobile bed, typical boundary layer velocity profiles were observed and significantly affected by the introduction of the model turbine, with an important overall velocity decrease. Recovery was observed to be much smaller than above the fixed bed and again varied laterally. Shear velocity profiles showed similar structure and magnitude with and without the rotor in the flume. The ripples that were clearly visible in the sediment bed in the absence of the rotor were affected by the wake and scour in a horse shoe shape developed by

the rotor presence, with deposition at the centreline. Sediment transport was higher on the negative side of the flume while in the positive some bedforms were still present. The experiments with the rotor at different heights from the bed resulted in deeper but more localised scour with the rotor closer to the bed and with no clear bedforms after the area of scour. Suspended sediment concentrations appeared to be enhanced near the bottom with the rotor in the flume, whereas decrease in sediment concentration in upper parts of the water column were found.

Several key consequences of the turbine in the flume have been identified. The flow suffers a decrease because of the loss of kinetic energy at the rotor location. Critically, the wake produced effects on the flow more than one diameter in the cross wise direction and more than 15 diameters in the streamwise direction, thus implying a much larger wake with slower recovery than when the rotor is outside the bottom boundary layer (fixed bed case). The wake is also developing in an asymmetric way along the flume. The near wake increased the bottom shear stress producing scour but also a deposition area at the centreline. This sediment transport at the bottom resulted in an almost flat bed over a limited section of the profile. The asymmetric flow field also resulted in an enhancement of the non-uniform distribution of the bottom morphology and sediment suspension patterns. The decrease in flow velocity and no wake recovery after 15 diameters could have an impact on the efficiency of turbine arrays while modifications to the sediment transport may have important effects on the environment. Even though the experiments were not scaled to marine dimensions, the study highlights important interactions between the flow, the sediment bed and a TST. More studies are needed to quantify the issues found in order to obtain the best turbine performance and diminish the environmental impact. Moreover, variable measurements should cover the entire field behind the turbine, i.e. near and far wake and stream and cross wise directions, to analyse the asymmetric behaviour found in this study.

Acknowledgments

The authors wish to acknowledge funding of the Engineering and Physical Sciences Research Council (EPSRC) to grant EP/J010359/1 Interactions of flow, tidal stream turbines and local sediment bed under combined waves and tidal conditions, which is part of the Supergen consortium. All data presented in this manuscript may be obtained from the authors. We also want to thank the anonymous reviewers for their important comments to improve this manuscript.

Appendix A. Supplementary data

Supplementary data related to this article can be found at https://doi.org/10.1016/j.renene.2018.05.094.

References

[1] R. Wengenmayr, T. Bührke, Renewable Energy: Sustainable Energy Concepts for the Energy Change, Wiley, 2012, ISBN 978-3-527-41187-0.
[2] M. Baeye, M. Fettweis, In situ observations of suspended particulate matter plumes at an offshore wind farm, southern north sea, Geophys. Marine Lett. 35 (2015) 247–255, https://doi.org/10.1007/s00367-015-0404-8.
[3] Q. Vanhellemont, K. Ruddick, Turbid wakes associated with offshore wind turbines observed with landsat 8, Rem. Sens. Environ. 145 (2014) 105–115, https://doi.org/10.1016/j.rse.2014.01.009.
[4] X. Li, M. Li, S.J. McLelland, L.B. Jordan, S.M. Simmons, L.O. Amoudry, R. Ramírez-Mendoza, P.D. Thorne, Modelling tidal stream turbines in a three-dimensional wave-current fully coupled oceanographic model, Renew. Energy 114 (2017) 297–307, https://doi.org/10.1016/j.renene.2017.02.033.
[5] L. Myers, A.S. Bahaj, Experimental analysis of the flow field around horizontal axis tidal turbines by use of scale mesh disk rotor simulators, Ocean Eng. 37 (2010) 218–227, https://doi.org/10.1016/j.oceaneng.2009.11.004.
[6] L. Chamorro, C. Hill, S. Morton, C. Ellis, R. Arndt, F. Sotiropoulos, On the interaction between a turbulent open channel flow and an axial-flow turbine, J. Fluid Mech. 716 (2013) 658–670, https://doi.org/10.1017/jfm.2012.571.
[7] F. Maganga, G. Germain, J. King, G. Pinon, E. Rivoalen, Experimental characterisation of flow effects on marine current turbine behaviour and on its wake properties, IET Renew. Power Gener. 4 (2010) 498–509, https://doi.org/10.1049/iet-rpg.2009.0205.
[8] L. Myers, A.S. Bahaj, Wake studies of a 1/30th scale horizontal axis marine current turbine, 34, 2007, pp. 758–762, https://doi.org/10.1016/j.oceaneng.2006.04.013.
[9] L. Myers, A.S. Bahaj, An experimental investigation simulating flow effects in first generation marine current energy converter arrays, Renew. Energy 37 (2012) 28–36, https://doi.org/10.1016/j.renene.2011.03.043.
[10] E. Foufoula-Georgiou, M. Guala, F. Sotiropoulos, Marine-hydrokinetic energy and the environment: observations, modelling, and basic processes, EOS 93 (2012) 111.
[11] T. Stallard, T. Feng, P. Stansby, Experimental study of the mean wake of a tidal stream rotor in a shallow turbulent flow, J. Fluid Struct. 54 (2015) 235–246, https://doi.org/10.1016/j.jfluidstructs.2014.10.017.
[12] N. Möller, H. Kim, V. Neary, M. García, L. Chamorro, On the near-wall effects induced by an axial-flow rotor, Renew. Energy 91 (2016) 524–530, https://doi.org/10.1016/j.renene.2016.01.05.
[13] C. Hill, M. Musa, L. Chamorro, C. Ellis, M. Guala, Local scour around a model hydrokinetic turbine in an erodible channel, J. Hydraul. Eng. 140 (2014), 04014037, https://doi.org/10.1061/(ASCE)HY.1943-7900.0000900.
[14] C. Hill, M. Musa, M. Guala, Interaction between instream axial flow hydrokinetic turbines and uni-directional flow bedforms, Renew. Energy 86 (2016) 409–421, https://doi.org/10.1016/j.renene.2015.08.019.
[15] A. Davies, P. Thorne, Advances in the study of moving sediments and evolving seabeds, Surv. Geophys. 29 (2008) 1–36, https://doi.org/10.1007/s10712-008-9039-x.
[16] D. Goring, V. Nikora, Despiking acoustic Doppler velocimeter data, J. Hydraul. Eng. 128 (2002) 117–126, https://doi.org/10.1061/(ASCE)0733-9429(2002)128:1(117).
[17] N. Mori, T. Suzuki, S. Kakuno, Noise of acoustic Doppler velocimeter data in bubbly flows, 133, 2007, pp. 122–125, https://doi.org/10.1061/(ASCE)0733-9399(2007)133:1(122).
[18] P. Bell, P. Thorne, Measurements of sea bed ripple evolution in an estuarine environment using a high resolution acoustic sand ripple profiling system, in: Proceedings of Oceans, vol. 97, MTS/IEEE, Washington D.C., 1997, pp. 339–343.
[19] B. Moate, P. Thorne, R. Cooke, Field deployment and evaluation of a prototype autonomous two dimensional acoustic backscatter instrument: the bedform and suspended sediment imager (BASSI), Continent. Shelf Res. 112 (2016) 78–91, https://doi.org/10.1016/j.csr.2015.10.017.
[20] P. Thorne, R. Meral, Formulations for the scattering properties of suspended sandy sediments for use in the application of acoustics to sediment transport processes, Continent. Shelf Res. 28 (2008) 309–317, https://doi.org/10.1016/j.csr.2007.08.002.
[21] S. Tedds, I. Owen, R. Poole, Near-wake characteristics of a model horizontal axis tidal stream turbine, Renew. Energy 63 (2014) 222–235, https://doi.org/10.1016/j.renene.2013.09.011.
[22] A. Singh, E. Foufoula-Georgiou, F. Porté-Agel, P. Wilcock, Coupled dynamics of the co-evolution of gravel bed topography, flow turbulence and sediment transport in an experimental channel, J. Geophys. Res. 117 (2012) 1–20, https://doi.org/10.1029/2011JF002323.
[23] S. Bennet, J. Best, Mean flow and turbulence structure over fixed, two-dimensional dunes: implications for sediment transport and bedform stability, Sedimetology 42 (1995) 491–513, https://doi.org/10.1017/jfm.2012.571.
[24] J. Best, The fluid dynamics of river dunes: a review and some future research directions, J. Geophys. Res. 110 (2005) 1–21, https://doi.org/10.1029/2004JF000218.